First-principles study of the adsorption of sulfur on Pt(111): S core-level shifts and the nature of the Pt-S bond

Zongxian Yang and Ruqian Wu*
Department of Physics and Astronomy, University of California, Irvine, California 92697-4575

Jose A. Rodriguez
Department of Chemistry, Brookhaven National Laboratory, Upton, New York 11973

(Received 10 August 2001; revised manuscript received 22 October 2001; published 28 March 2002)

The adsorption of a sulfur atom and a sulfur molecule on the Pt(111) surface is investigated through the first-principles full-potential linearized augmented plane-wave (FLAPW) and pseudopotential calculations. Different sulfur coverages (0.25, 0.33, and 1 ML) and several adsorption geometries are considered. It is found that, for atomic sulfur, the S-Pt bond is weakened with the increase of sulfur coverage and the most stable adsorption site changes from fcc-hollow site to atop site. The S $2p$ core levels shift to higher binding energy with the increase of S coverage. The Pt $4f$ core levels are stabilized upon interaction with the S adsorbate, and yet the Pt to S charge transfer is not substantial in many cases. S adsorption induces significant decreases in the density of Pt $5d$ states near the Fermi energy. For the case of S_2 adsorption, the S-S bond length is 2.1 Å with one atom near an atop position and the other on a mixed bridge-hollow site. The adsorption energy is close to 44 kcal/mol.

DOI: 10.1103/PhysRevB.65.155409 PACS number(s): 68.43.−h, 82.65.+r

I. INTRODUCTION

Platinum is widely used as a catalyst in the chemical and petrochemical industries due to its peculiar properties.[1,2] Its catalytic lifetime, however, is limited by many factors: chief among them is sulfur poisoning.[1–6] Millions of dollars are lost every year in industrial applications as a consequence of the negative effects of sulfur poisoning on the activity and/or selectivity of Pt catalysts.[1,4,5] At the present stage the mechanism responsible for sulfur poisoning is not fully understood.[4–6] The reduction in activity or selectivity induced by sulfur could result from modifications in the morphology of the catalyst, steric blocking of reaction pathways, and changes in the electronic properties of the active sites.[4,6] To minimize the negative effects of sulfur poisoning, one needs a fundamental understanding of the nature of the Pt-S bond.

The adsorption of sulfur on Pt(111) was studied by Rodriguez *et al.*[7] using photoemission and thermal desorption mass spectroscopy (TDS) as well as a first-principles pseudopotential method. It was found that the bonding properties of sulfur to Pt(111) strongly depended on the coverage of the adsorbate. The Pt-S interactions were substantially weakened with the increase of sulfur coverage. For coverages of S higher than 0.4 monolayer (ML), desorption of S_2 species was observed in TDS and the S $2p$ core levels substantially shifted in binding energy. This phenomenon is illustrated by the high-resolution photoemission data shown in Fig. 1. At small S coverage (0.15 ML), a well-defined doublet is seen in the S $2p$ region arising from S atoms bonded to fcc-hollow sites of the Pt(111) surface.[7,8] As the coverage of sulfur increases on the surface (>0.3 ML), new features appear in the S $2p$ spectra. The spectrum for 0.93 ML of sulfur contains contributions from two different types of sulfur species (*a* and *b* in Fig. 1), with S $2p3/2$ binding energies that are 0.8–1.0 eV different. Such large core-level shifts, if they come from initial state effects,[9] would suggest important changes in the nature of the Pt-S bond as a function of sulfur coverage. While the first-principles pseudopotential results in Ref. 7 helped the interpretation of experimental data, the core-level shifts were not available. Photoemission spectra for the adsorption of sulfur on W(100) (Ref. 10), Rh(111) (Ref. 11), and Pd(111) (Ref. 12) also exhibit big changes in the S $2p$ positions with coverage. Again, the phenomenon is poorly understood.[10–12] In general terms, it is important to establish if initial-state effects can cause this type of core-level shifts for adsorbed sulfur.

In this study, the all-electron full-potential linearized augmented plane-wave (FLAPW) method[13] is used to study the adsorption of sulfur on a Pt(111) surface. The same system is investigated using first-principles pseudopotential methods[14,15] and a series of different exchange-correlation functionals.[16–18] Following this approach, we are able to obtain general trends with theoretical methods that use different levels of approximation. While we find that most results of the FLAPW method agree with those obtained through pseudopotential calculations, some significant deviation also exist, especially for the values of adsorption energies. Nevertheless, trends in the relative stabilities of the adsorption sites and variations in the strength of the S-Pt interactions with S coverage are identical in the all electron and pseudopotential calculations. The FLAPW calculations indicate that the S $2p$ core levels are very sensitive to changes in S coverage and adsorption sites. Thus, initial state effects could play a major role in the core-level shifts of Fig. 1.

II. MODELS AND COMPUTATIONAL METHODS

A. Pseudopotential calculations

The pseudopotential calculations were carried out using the CASTEP (Cambridge Serial Total Energy Package) suite of

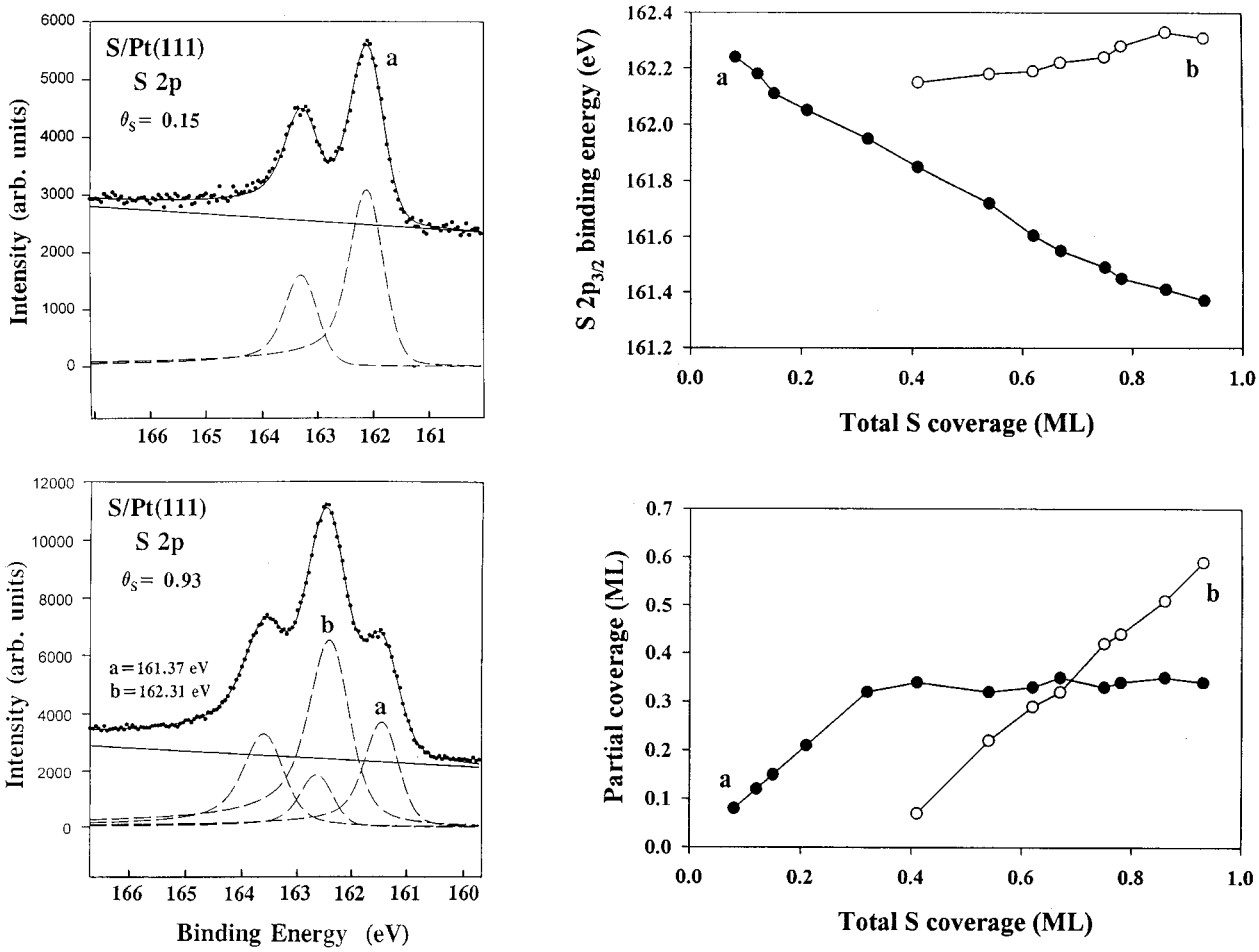

FIG. 1. High-resolution S $2p$ photoemission spectra for the adsorption of 0.15 and 0.93 ML of sulfur on Pt(111). The spectra were fitted using a many-body line shape (Doniach-Sunjic) convoluted with a Gaussian function to account for instrumental resolution. Right side: variation of the S $2p_{3/2}$ binding energy and partial coverage of the *a* and *b* species with total sulfur coverage.

programs.[14] The wave functions of valence electrons were expanded in a basis set of plane waves with kinetic energy up to a cutoff value of 25 Ry. The effect of tightly bound core electrons was represented by nonlocal ultrasoft pseudopotentials of the form suggested by Vanderbilt.[15] Reciprocal-space integration over the Brillouin zone was approximated through a careful sampling at a finite number of k points using the Monkhorst-Pack scheme.[19] Up to 81 special k points were considered for Brillouin zone sampling and integration. In these calculations, the kinetic energy cutoff and the density of the Monkhorst-Pack k-point mesh were chosen well above the minimum values necessary to ensure convergence of the computed structures and energetics. The exchange-correlation contribution was treated in the generalized gradient approximation (GGA) with three different functionals: Perdew-Wang (PW91),[16,20] Perdew-Burke-Ernzerhof (PBE),[17] and a revised version of Perdew-Burke-Ernzerhof (RPBE).[18,21]

The structural parameters of the S/Pt(111) system in its different configurations were determined using the Broyden-Fletcher-Goldfarb-Shanno (BFGS) minimization technique, with the following thresholds for the converged structures: energy change per atom less than 5×10^{-6} eV, residual force less than 0.02 eV/Å, and the displacement of atoms during the geometry optimization less than 0.001 Å. The fcc lattice constants obtained for bulk Pt with the PW91 (3.992 Å), PBE (4.007 Å), and RPBE (4.005 Å) functionals are very similar to those obtained in other theoretical studies (3.97–4.02 Å) (Refs. 22 and 23) and the experimental value (3.924 Å) (Ref. 23) Due to computational requirements, the thickness of the resulting slab in most of the pseudopotential studies was limited to six atomic layers. The two-dimensional periodic slab was then embedded in a three-dimensional periodic supercell, with a vacuum of 12 Å thick separating the top of the slab and the bottom of its periodic image. This large vacuum width should be more than enough to prevent interactions between neighboring slabs. The CASTEP calculations predicted almost no relaxation of the clean Pt(111) surface with respect to the (111) face of bulk Pt, in agreement with experimental investigations.[7] Sulfur was adsorbed on one side of the slab, S $p(1\times1)$ and S $p(2\times2)$ superstructures, and the geometry of the adlayer and first two Pt layers was fully relaxed, while the four bottom Pt layers were frozen at the bulk crystalline spacings in order to mimic the presence of a semi-infinite crystalline

material beneath the surface. The adsorption energy of surfur is defined as $E_{ad}=E_{Pt(111)}+E_S-E_{S/Pt(111)}$, with $E_{S/Pt(111)}$, $E_{Pt(111)}$, and E_S representing the total energies of the adsorbed system, the clean Pt(111) surface, and a free S atom, respectively. In test studies, we investigated the adsorption of 1 ML of S on Pt(111) using eight- and six-layer slabs and obtained almost identical results. For the systematic work reported in Sec. III, a six-layer slab has been used owing to the computer time required by the calculations. Some significant differences were found when comparing the results obtained with a eight-layer slab and four- or three-layer slabs used in previous pseudopotential calculations for the S/Pt(111) system.[7,24]

B. FLAPW calculations

The film version of the FLAPW method used here[13] has no shape approximation for charge, potential, and wave functions in the muffin-tin, interstitial, and vacuum regions. A single slab geometry is used to simulate the surfaces with an infinitely extended vacuum on each side. The real space is divided into three different regions: namely, muffin-tin (MT) spheres around the nuclei, a vacuum region on each side of the slab, and the remaining interstitial region. The wave function, charge density, and the effective single-particle potential are represented by a ''natural'' representation in each of the three spatial regions without any shape approximation in the whole space. Compared to the pseudopotential CASTEP approach, the FLAPW approach avoids the three basic approximations: namely, (1) the frozen core, (2) ''pseudizing'' the ionic potential and thereby removing the near-nucleus wave function nodes, and (3) approximation or neglecting of the nonlinearity of the core-valence exchange correlation interaction. In addition, relativistic effects (except the spin-orbit coupling for the valence electrons) are explicitly invoked in the LAPW bases and Hamiltonian. Therefore, FLAPW calculations are expected to be more accurate, especially when heavy elements (e.g., Pt here) are involved.

The GGA (in the form of PBE96) (Ref. 17) is adopted to describe the exchange-correlation interactions. In the muffin-tin region, spherical harmonics with a maximum angular momentum of 8 are used to expand the charge, potential, and wave functions. In the interstitial region, plane waves with energy cutoffs of 225 Ry (for the charge and potential) and 16 Ry (for the variational bases) were employed. Up to 37 special *k* points in the irreducible two-dimensional Brillouin zone are used for integrals in the reciprocal space.[25] Test calculations for atop site adsorption on a $p(1\times1)$ surface of Pt(111) with more *k* points and larger energy cutoffs showed that this approach is reasonable for the convergence of structure and total energy.

The Pt substrate is modeled by a five-layer Pt(111) slab. A sulfur atom or a sulfur molecule is placed on each side of the slab to retain the inversion symmetry. In this case, the adsorption energy of sulfur is defined as $E_{ad}=\frac{1}{2}(E_{Pt(111)}+2E_S-E_{S/Pt(111)})$, with $E_{S/Pt(111)}$, $E_{Pt(111)}$, and E_S representing the total energies of the adsorbed system, the clean Pt(111) surface, and a free S atom, respectively. Different sulfur coverages (1/3 ML and 1 ML) and different adsorption geometries (atop, bridge, hcp-hollow, and fcc-hollow adsorption sites) are considered. The equilibrium structures for the adlayers were determined using total energy minimization guided by atomic forces[26] with a criterion that required the force on each atom to be less than 0.02 eV/Å.

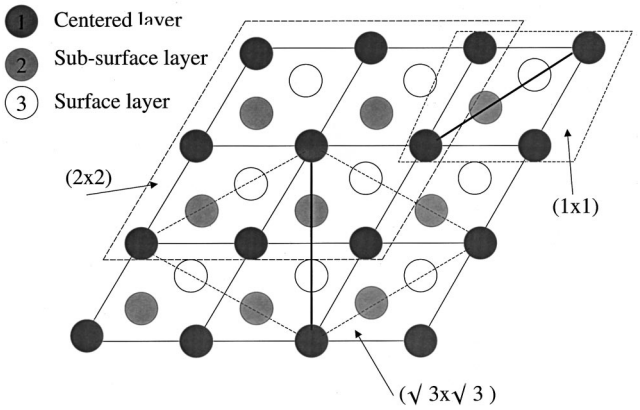

FIG. 2. Schematic top view of a Pt(111) surface. A $p(1\times1)$, a $p(2\times2)$, and a $(\sqrt{3}\times\sqrt{3})$ unit cell are shown by dotted lines.

III. RESULTS AND DISCUSSION

A. Energetic properties for different adsorption geometries

We will begin by discussing the results for the all-electron calculations. The schematic top views of different unit cells [$p(1\times1)$, $p(2\times2)$, and $p(\sqrt{3}\times\sqrt{3})$] on a Pt(111) surface are shown in Fig. 2. For the $p(\sqrt{3}\times\sqrt{3})$ cell with S adatoms (coverage $\theta=1/3$), the in-plane symmetry becomes very low. As listed in Table I, the adsorption energies are 67.8 kcal/mol, 100.3 kcal/mol, 109.5 kcal/mol, and 113.9 kcal/mol for the atop, bridge, hcp-hollow, and fcc-hollow, respectively (1 kcal/mol = 0.0424 eV/adatom). The sequence of the adsorption energies, i.e., E_{ad}(atop)$<E_{ad}$(bridge)$<E_{ad}$(hcp-hollow)$<E_{ad}$(fcc-hollow), is the same as given by pseudopotential calculations for the $\theta=1/4$ case [with a

TABLE I. Adsorption energies and bond lengths of atomic and molecular sulfur on Pt(111): FLAPW(GGA) results.

Atoms	$d_{Pt\text{-}S}$ (Å)	E_{ad} (kcal/mol)
$p(\sqrt{3}\times\sqrt{3})R30°$, 1/3 ML atomic S		
Atop	2.25	67.8
Bridge	2.31	100.3
h-hcp	2.40	109.5
h-fcc	2.38	113.9
$p(1\times1)$, 1.0 ML atomic S		
Atop	2.32	79.7
Bridge	2.60	64.9
h-hcp	2.65	64.5
h-fcc	2.63	66.9
$p(1\times\sqrt{3})$, 1.0 ML S (molecule adsorption)		
$d_{S\text{-}S}$	2.12	79.1
$d_{S\text{-}Pt(atop)}$	2.39	
$d_{S\text{-}Pt(mix)}$	2.92	

TABLE II. Adsorption energies and bond lengths of S-(2×2) on Pt(111): pseudopotential (GGA) results.

	$d_{Pt\text{-}S}$ (Å)			E_{ad} (kcal/mol)		
Functionals	PW91	PBE	RPBE	PW91	PBE	RPBE
Atop	2.19	2.18	2.19	64.6	53.2	51.3
Bridge	2.25	2.25	2.25	72.3	66.8	60.5
h-hcp	2.28	2.29	2.29	85.4	80.7	75.6
h-fcc	2.29	2.29	2.28	89.8	85.1	79.7

$p(2\times2)$ adsorption structure; see below]. The most stable adsorption site is over the fcc-hollow site, where E_{ad} is as large as 113 kcal/mol and the nearest S-Pt bond length is 2.38 Å. This result agrees well with a quantitative low-energy electron diffraction (LEED) measurement,[8] which indicated that S adatoms prefer the fcc-hollow site on Pt(111) at small coverage. The least favorable adsorption site is the atop site, where the adsorption energy is only 67.8 kcal/mol and the S-Pt bond length is 2.25 Å. As expected, the difference between E_{ad}(hcp-hollow) and E_{ad}(fcc-hollow) is very small (<4.5 kcal/mol). This indicates that the second-neighbor interaction between S and Pt is weak, but not negligible. The calculated bond length (2.38 Å) is about 4%–5% larger than the experimental value (2.28 ± 0.03 Å) and the calculated binding energy (113.9 kcal/mol) is also significantly larger than the measured results through TDS (75 kcal/mol).[7]

Table II lists the results of pseudopotential calculations for 0.25 ML of S on Pt(111), S $p(2\times2)$ superstructure. For the three exchange-correlation functionals examined the trends are identical and corroborate those seen in the FLAPW calculations for a S $p(\sqrt{3}\times\sqrt{3})$ superstructure. Independently of the exchange–correlation functional employed, S adsorption on a fcc-hollow site appears as the most stable configuration, in agreement with the results of LEED.[8] The calculated S-Pt bond distances (2.28–2.29 Å) are close to those found in LEED (2.28 Å),[8] cluster calculations (2.24–2.33 Å),[24,27] and in a three-layer slab study performed also with the PBE functional but with a different pseudopotential (2.25 Å).[24] For the PBE functional the predicted S binding energy on a fcc-hollow site (85 kcal/mol) is bigger than that measured in TDS experiments (75 kcal/mol),[7] but smaller than those found in the pseudopotential calculations of Ref. 24 (105 kcal/mol) or in the FLAPW results of Table I (113 kcal/mol). These discrepancies probably originate in the different approximations used for each set of calculations (see Sec. II above). If theoretical methods with similar approximations are used, pseudopotentials can give results similar to those of FLAPW, but this may not be necessarily the case when comparing predictions of different types of codes.[22] Cluster calculations with different levels of theory[24,28] give S adsorption energies that range from 80 to 115 kcal/mol. In Table II, the absolute values for the S adsorption energies significantly change from one functional to another. In general, the RPBE functional predicts S binding energies that are smaller than those predicted by the PW91 or PBE functionals. This is consistent with trends found in theoretical studies for other adsorbates.[18,21]

TABLE III. Adsorption energies and bond lengths of atomic and molecular sulfur on Pt(111): pseudopotential (GGA) results.

	$d_{Pt\text{-}S}$ (Å)			E_{ad} (kcal/mol)		
Functionals	PW91	PBE	RPBE	PW91	PBE	RPBE
$p(1\times1)$, 1.0 ML atomic S						
Atop	2.29	2.28	2.29	57.9	52.6	49.3
Bridge	2.37	2.35	2.36	54.8	48.7	46.1
h-hcp	2.43	2.42	2.43	46.8	43.6	39.4
h-fcc	2.42	2.41	2.42	51.6	47.5	43.3
$p(1\times\sqrt{3})$, molecular adsorption						
$d_{S\text{-}S}$	2.01	2.02	2.01	60.9	56.9	53.7
$d_{S\text{-}Pt(atop)}$	2.32	2.29	2.29			
$d_{S\text{-}Pt(mix)}$	2.46	2.40	2.41			

The S/Pt(111) systems examined in Refs. 24 and 28 and above contain a limited amount of sulfur on the metal surface. Table I shows FLAPW results for the adsorption of a full layer of atomic S [$\theta=1$, with a $p(1\times1)$ superstructure]. As the sulfur coverage raises from 1/3 to 1 ML, the adsorption energy decreases sharply by 35%–41% for the bridge and two hollow sites. By contrast, E_{ad}(atop) is enhanced by about 18% when the S coverage increases. Dramatically, the atop site becomes the most favorable one among the four adsorption sites for 1.0-ML atomic S adsorption. An identical conclusion can be reached after analyzing the corresponding results of pseudopotential calculations in Table III. TDS data for S/Pt(111) show a substantial decrease in the S adsorption energy with increasing adsorbate coverage, and the photoemission results in Fig. 1 suggest that there could be a change in adsorption site.[7] In Tables I–III, the weakening of the Pt-S interactions is accompanied by a large elongation (up to 0.2 Å) of the S-Pt bond distances.

Clearly, both the adsorption energy and bond length depend sensitively on the coverage, adsorption site, and even the local arrangement of adsorbates. This can be used to explain the deviations between the measured and calculated adsorption energies, since the atomic arrangements in the experiments may not be as ideal as in the theoretical models. In addition, S adatoms may form S_2 molecules on Pt(111).[7] Using a $p(1\times\sqrt{3})$ surface unit cell as shown in Fig. 3 ($\theta=1$) with S_2 adsorbates, the adsorption energy for a S_2 molecule is found to be 79.1 kcal/mol (including the S-S binding energy since the single S atom is used as the reference). This value is very slightly smaller than that for the atomic adsorption case (79.7 kcal/mol), indicating that both adsorption phases may coexist at the high-coverage regime. If one uses a free S_2 molecule as the reference (simulated by a freestanding S_2 lattice with a large separation), the molecular adsorption energy for S_2/Pt(111) is 44.3 kcal/mol, a value which agrees very well with the experimental results (~45 kcal/mol).[7] The pseudopotential calculations in Table III also predict similar adsorption energies for S_2 and 2S species on Pt(111) at $\theta=1$. This is valid for all the examined exchange-correlation functionals. When comparing the all-electron and pseudopotential calculations with the PBE functional, the molecular adsorption energies are quite close to

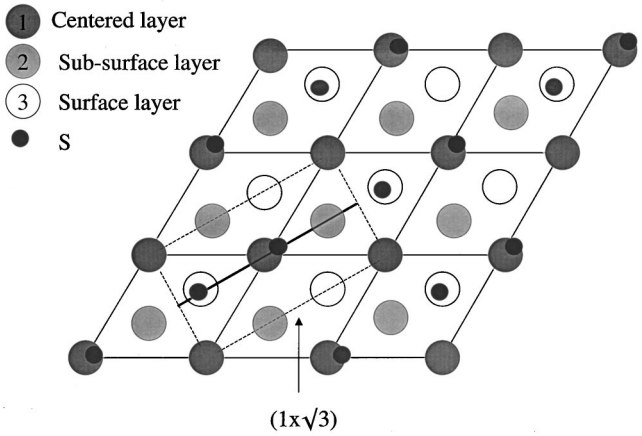

FIG. 3. Schematic top view for 1 ML of S_2 on a Pt(111) surface. A $(1\times\sqrt{3})$ unit cell is shown by dotted lines.

each other: 39.1 kcal/mol from the pseudopotential approach versus 44.3 kcal/mol from the FLAPW approch. For the S_2 adsorption case, one S atom locates near the atop position (S_{atop}) and the other on a mixed hollow-bridge site (S_{mix}); see Fig. 3. In the FLAPW calculations (Table I), the S-S bond length is 2.12 Å, while the nearest S-Pt bond distances are 2.39 Å (atop) and 2.92 Å (mix), respectively. The S-S and S-Pt bond lengths calculated with the pseudopotential approach (Table III) are somewhat smaller than those from the FLAPW method.

The all-electron and pseudopotential calculations described above indicate that the behavior of the S/Pt(111) system can be very complex. Changes in the sulfur coverage can lead to a movement of the adsorbate from one surface site to another and the existence of S-S bonding. In the following sessions, we will examine how these transformations affect the nature of the S-Pt bond and the core levels of sulfur.

B. Electronic structure and bonding mechanisms

Figure 4 shows valence photoemission spectra for several coverages of sulfur on Pt(111)and platinum sulfide.[27] The deposition of sulfur (i.e., formation of Pt-S bonds) induces a decrease in the density of states of the Pt $5d$ band near the Fermi level. This electronic perturbation was studied in detail with the FLAPW method and a five-layer slab. The calculated layer-projected density of states (LP-DOS, obtained from the summation of atomic DOS in each atomic layer) indicates that the adsorption of S on the Pt(111) surface has a very minor influence on the electronic structures of the center and even subsurface Pt layers. Therefore our five-layer model for the Pt(111) substrate is reasonably thick. The DOS projected on the surface Pt layer are displayed in Figs. 5 and 6 for the 1/3 ML and 1 ML atomic S adsorption, respectively. The DOS for the S atom are shown by the dashed lines, while the surface layer DOS for the clean Pt(111) surface are also shown in each panel by the dotted lines. The strength of the S-Pt hybridization (characterized by the S-induced change in Pt-DOS) clearly determines the value of E_{ad} for each case. For the $p(\sqrt{3}\times\sqrt{3})$ geometry, S adsorption broadens the Pt $5d$ band and drastically lowers the value of the

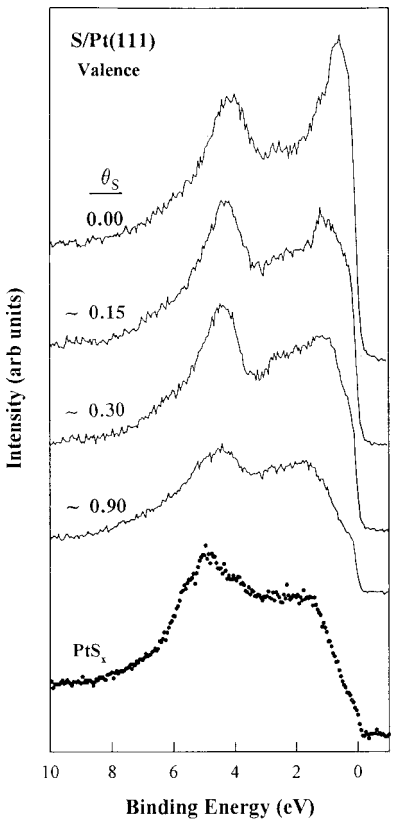

FIG. 4. Valence photoemission spectra for clean Pt(111) and S/Pt(111) surfaces. At the bottom (dotted trace), for comparison, is shown the corresponding spectrum for platinum sulfide.

DOS at the Fermi level, especially for adsorption on the fcc- and hcp-hollow sites. The least change in DOS occurs for the atop site adsorption, which corresponds to the least favorable configuration at low S coverages (cf. Tables I and II). In contrast, for the $p(1\times1)$ geometry, the largest decrease of the DOS at E_F occurs for the atop site case, Fig. 6. At this high coverage, the S-Pt hybridization is strong for all the cases. The S-induced decreases in the DOS at E_F for the bridge, hcp-hollow, and fcc-hollow site adsorption are very close to each other. It is thus understandable that they have almost the same adsorption energies at $\theta=1$ (cf. Tables I and III). As expected, the S s,p band spreads over a wide energy range due to the large spatial extension of the s-p atomic orbits.

To elucidate more clearly, the calculated valence charge density differences on the vertical cross section (passing through the thick solid line shown in Fig. 2) $[\Delta\rho=\rho(\mathrm{S/Pt})-\rho(\mathrm{S})-\rho(\mathrm{Pt})$, where $\rho(\mathrm{S/Pt})$, $\rho(\mathrm{S})$, and $\rho(\mathrm{Pt})$ are the charge densities for the adsorbed system, the freestanding S monolayer, and the clean Pt substrate] for the four adsorption sites are presented in panels (atop), (bri), (hcp), and (fcc) of Fig. 7 (for $\theta=1/3$) and Fig. 8 (for $\theta=1$), respectively. Their planar averages are also given in Fig. 9 (for $\theta=1/3$) and Fig. 10 (for $\theta=1$). Significant differences can be found for the two coverages. The S adatoms are almost not ionic at all for $\theta=1/3$. In the pseudopotential calculations of Table II, $\theta=1/4$, a Mulliken population analysis[29] gave very small ($<0.15e$) charge separations, and the S-Pt bond is best de-

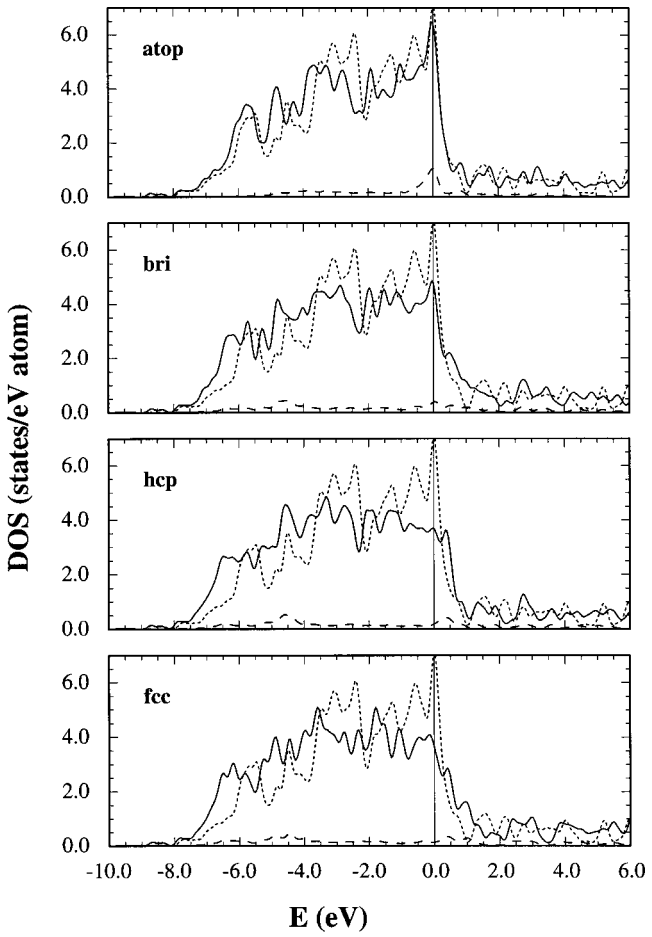

FIG. 5. The DOS projected on the surface Pt layer (SDOS) for 1/3 ML atomic S adsorption (solid curves), accompanied by the SDOS for the clean Pt(111) surface (dotted curves). The dashed curves represent the DOS of the S adatom. The vertical line at $E=0$ represents the Fermi level. Calculated with the FLAPW method.

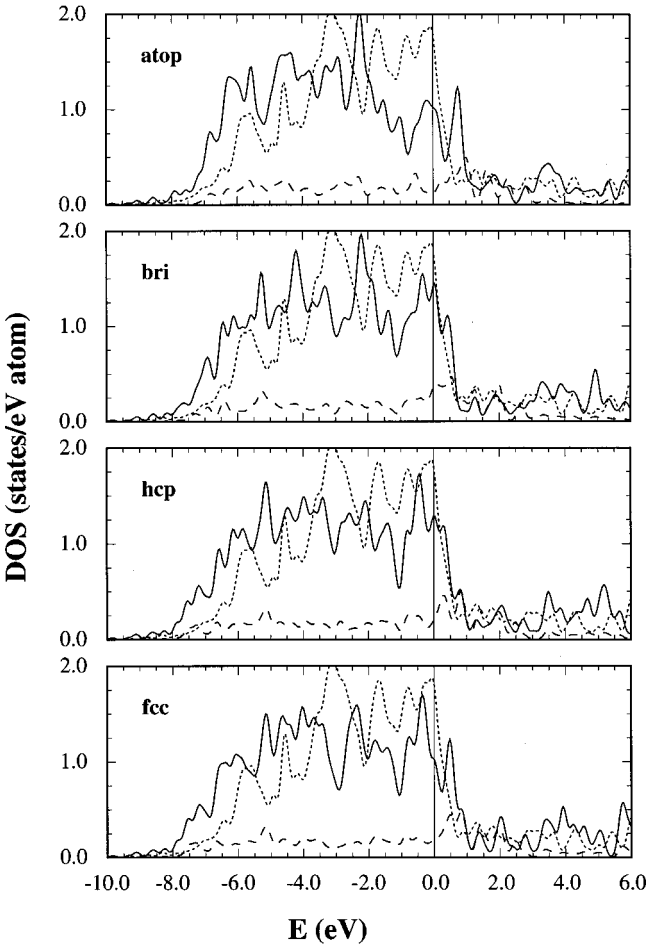

FIG. 6. The same as in Fig. 5, but for 1 ML atomic S adsorption.

scribed as covalent. Cluster calculations for small coverages of S on Pt(111) also show a low degree of ionicity in the S-Pt bond.[27] A very interesting situation is seen in Fig. 8 for 1 ML of S on Pt(111), where a substantial charge accumulation (or charge polarization from Pt towards S) occurs. Consequently, repulsive forces among the S ions could reduce the adsorption energies in the high-coverage case. However, the behavior of the system is more complex than this since, to compensate for the weakening of the S-Pt bonds, S-S bonds can be formed. Independently of this, a strong S-Pt hybridization is always observed. From the similarity in the profiles (panel ''S2'' and panel ''atop'') of the planar-average charge density difference in Fig. 10, one can find that the S-Pt interaction in the molecular configuration is mainly due to the atop S adatom.

For the charge contours of Figs. 7 and 8, electrons are depleted from the area right under the S adatom for the hcp-hollow configuration. This suggests that the S and the underneath Pt are repulsive to each other and thus the hcp-hollow adsorption is less stable than the fcc-hollow one. For all the cases, the charge density around the center Pt atom remains almost intact.

In summary, the theoretical results discussed in this section indicate that the formation of S-Pt bonds induces a significant reduction in the density of states of Pt near the Fermi level, a phenomenon that may or may not be associated with a charge transfer depending on the sulfur coverage and adsorption site. The drop in the density of states of Pt should hinder the ability of this metal to interact with adsorbates,[30–32] leading to a decrease in its catalytic activity.[6,27]

C. Initial-state core-level shifts

As shown in Fig. 1, the line shape of the S $2p$ spectra for S/Pt(111) surfaces depends strongly on sulfur coverage. A similar trend is observed in photoemission data for sulfur on other metal surfaces.[10–12] It is not clear what causes the shifts in the S $2p$ core levels and, in particular, if the shifts come from initial-state effects.[9,7,27] In general, binding-energy shifts in core-level photoemission can be a consequence of initial state effects (i.e., real variations in the position of the core level produced by charge transfer, orbital rehybridization, volume perturbations, changes in chemical environment, etc.) and/or final-state effects (i.e., ''artifacts'' produced by changes in the screening of the core hole).[9,33] The

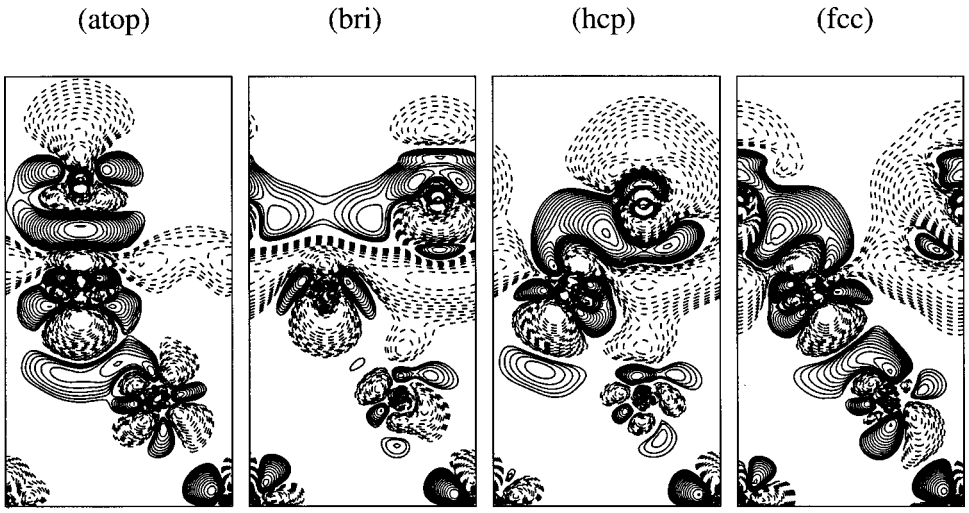

FIG. 7. The calculated charge density difference for the case of 1/3 ML atomic S adsorption. Contours are shown in the vertical cross section passing the thick solid line shown in Fig. 1 and start from $\pm 5\times 10^{-4}$ e/a.u.^{3} and increase successively by a factor of $10^{1/10}$. Dashed lines indicate negative differences. From FLAPW calculations.

FLAPW method is ideal for addressing this issue.[34] The method does not give the final-state contribution to the experimental core-level shifts (a more sophisticated theoretical treatment is necessary to obtain this[35,36]), but it allows us to study core-level positions as a function of the chemical environment (initial-state effects).[34] Our objective is a qualitative interpretation for the site dependence of experimental core-level shifts seen in Fig. 1.

The energies of the core states of the adsorbate (S $2p_{1/2}$, S $2p_{3/2}$) and those of the surface Pt atoms (Pt $4f_{5/2}$, Pt $4f_{7/2}$) with respect to the corresponding Fermi level for different coverages and adsorption sites are listed in Table IV. Clearly, the energies of the S $2p_{1/2}$ and S $2p_{3/2}$ core levels are very sensitive to the environment and the binding-energy shifts in Fig. 1 probably reflect initial-state effects. For $\theta=1/3$, the S adatoms on the hcp-hollow sites have the highest S $2p_{1/2}$ and S $2p_{3/2}$ binding energies, while they are reduced by 1.15 eV for the atop configuration. For $\theta=1$, the variation in the S core-level binding energy is less pronounced. The maximum difference (0.31 eV) occurs between the hcp-hollow and the atop configurations.

In addition, we found that the S $2p$ core-level energies are enhanced with an increase of S coverage. Dramatically, the core-level binding energies for the two most stable configurations (fcc-hollow for $\theta=1/3$, atop for $\theta=1$) are almost identical. This makes difficult an explanation of the experimental data in Fig. 1 without the aid of the first-principles results. For the adsorption of the S_2 molecule ($\theta=1$), the splitting between the core levels of the two S atoms is 0.23 eV.

Several useful conclusions can be reached after analyzing the results in Table IV and comparing them to existing S $2p$ photoemission spectra for the S/Pt(111) system.[7,27] At moderate S coverages and low temperatures, the S/Pt(111) system exhibits metastable states with S $2p$ binding energies smaller than that seen for a stable $p(\sqrt{3}\times\sqrt{3})$ superstructure.[7,27] According to Tables I and IV, these metastable states probably correspond to S atoms bonded to atop or bridge sites. Under these conditions there is a direct relationship between the strength of the S-Pt bond and the position of the S $2p$ core levels. The S $2p$ core-level shifts simply reflect variations in the electron distribution around S in each site and not necessarily a Pt to S charge transfer. For large coverages of S, two processes occur that can modify the position of the S core levels by initial-state effects: changes in the relative stability of the adsorption site and the

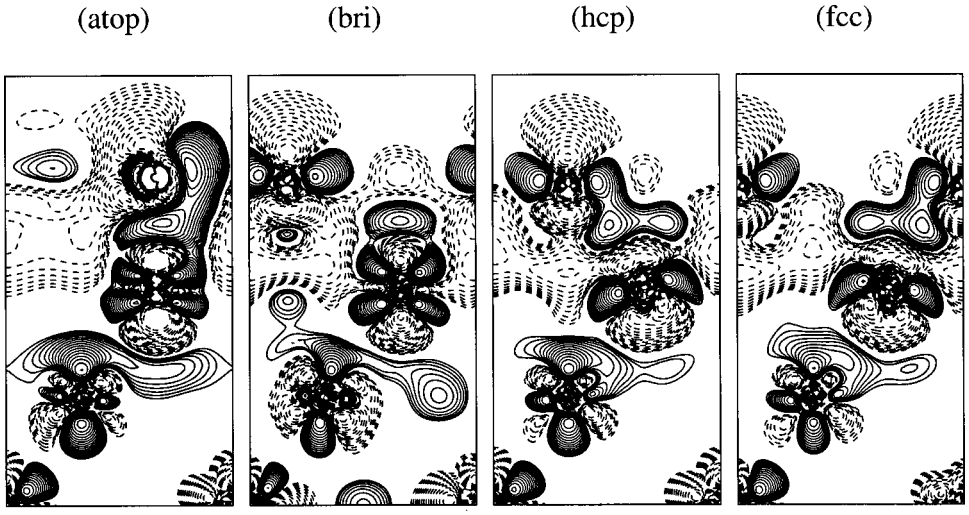

FIG. 8. The same as in Fig. 7, but for the case of 1 ML atomic S adsorption.

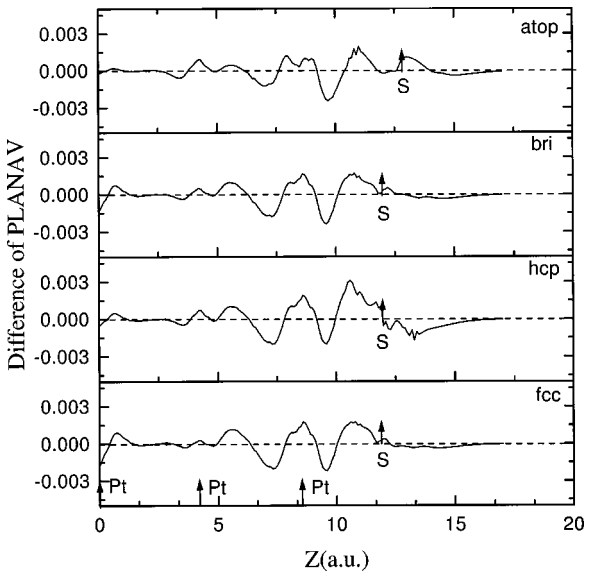

FIG. 9. The planar average charge density difference for the case of 1/3 ML atomic S adsorption on the plane perpendicular to the surface normal, which shows the change in charge distribution along the surface normal caused by the adsorption of S. Calculated with the FLAPW method.

existence of S-S bonds. The behavior seen in Fig. 1 for the S $2p_{3/2}$ binding energies of the species *a* probably reflects a change in the adsorption site of atomic S (hollow→bridge or atop). In Table IV, if one compares the S $2p$ position for the most stable configuration in the $p(\sqrt{3}\times\sqrt{3})$ superstructure (i.e., hollow-fcc site) and for the adsorbed S_2 molecule, there is an effective increase in the stability of the S $2p$ core levels. This is the trend observed in photoemission experiments for sulfur on Pt(111),[7,27] Rh(111),[11] Pd(111),[12] and Au(111),[37] when S_2 appears on the surface. In qualitative terms, the FLAPW calculations indicate that the measured S $2p$ shifts reflect changes in the initial state, although final-state effects can also contribute to them. It is difficult to offer a quantitative interpretation of the S $2p$ spectra in Fig. 1 at high S coverages, because for these coverages the surface contains a disordered mixture of sulfur species[7,27] and not the well-defined superstructures of Table IV.

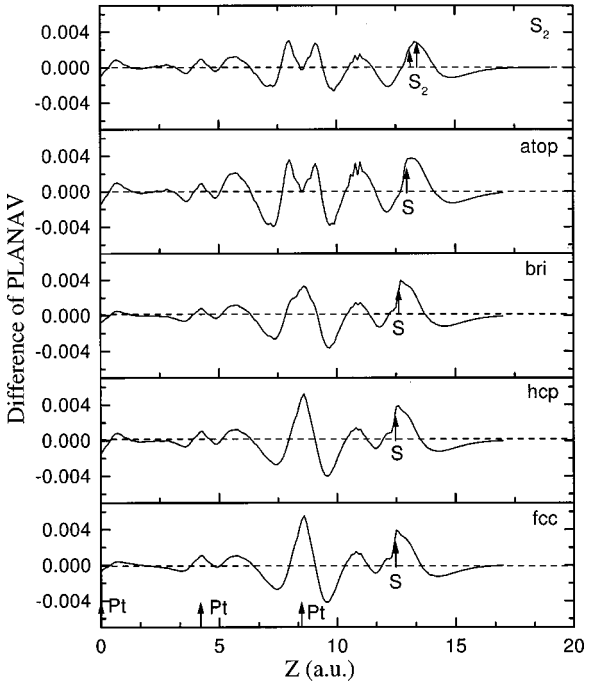

FIG. 10. The same as in Fig. 9, but for the case of 1 ML of atomic S or molecular adsorption.

TABLE IV. Core levels of adsorbed S and surface Pt. Pt_1 and Pt_2 represent two kinds of nonequivalent Pt atoms on the $p(\sqrt{3}\times\sqrt{3})$ $R30°$ surface with Pt_1 being the nearest neighbor of the adsorbed S atom.

Atoms	Sulfur	Surf-Pt_n	
	S $2p_{1/2}$ S $2p_{3/2}$	Pt $4f_{5/2}$	Pt $4f_{7/2}$
cln Pt(111)		−68.25	−64.79
$p(\sqrt{3}\times\sqrt{3})R30°$, 1/3 ML atomic S			
Atop	-151.39 -150.13	Pt_1: -69.05	-65.59
		Pt_2: -68.16	-64.70
Bridge	-152.22 -150.96	Pt_1: -68.74	-65.28
		Pt_2: -68.28	-64.82
h-hcp	-152.54 -151.27	-68.71	-65.25
h-fcc	-152.46 -151.19	-68.67	-65.20
$p(1\times1)$, 1.0 ML atomic S			
Atop	-152.46 -151.20	-69.09	-65.63
Bridge	-152.65 -151.39	-68.86	-65.40
h-hcp	-152.77 -151.51	-68.90	-65.44
h-fcc	-152.75 -151.48	-68.88	-65.42
$p(1\times\sqrt{3})$, 1.0 ML S (molecule adsorption)			
Atop	-152.63 -151.36	-68.78	-65.32
Mix	-152.40 -151.14	-68.46	-65.00

In Table IV, the core levels (Pt $4f_{5/2}$, Pt $4f_{7/2}$) of the surface Pt atom nearest to the S adatom are found to shift down by 0.42–0.8 eV for $\theta=1/3$ and by 0.63–0.84 eV for $\theta=1$ compared to those on the Pt(111) clean surface. For the adsorption of the S_2 molecule ($\theta=1$), the Pt $4f$ core levels are stabilized by 0.53 eV (0.23 eV) for the one near to the atop (mixed hollow-bridge) S adatom. The most pronounced energy shift occurs for the atop configuration either for lower ($\theta=1/3$) or higher ($\theta=1$) coverage. For the low coverage, the core levels of the surface Pt atoms that are not near the S adatom (Pt_2 in our notation) are perturbed very slightly: destabilized by 0.09 eV (atop configuration) or stabilized by 0.03 eV (bridge configuration), indicating that the S-Pt interaction is quite localized. It is interesting that for a $p(\sqrt{3}\times\sqrt{3})$ superstructure the Pt to S charge transfer is minimal (see above), but yet there are substantial shifts in the Pt $4f$ levels. In experiments of core-level photoemission, the sulfidation of Pt induces positive binding-energy shifts in the Pt $4f$ levels,[38] which according to our results probably originate in initial-state effects.

IV. SUMMARY

The adsorption of a sulfur atom and a sulfur molecule on the Pt(111) surface was investigated using the first-principles

FLAPW and pseudopotential calculations. Different sulfur coverage (1/4, 1/3, and 1 ML) and several adsorption geometries were considered. It was found that, for atomic sulfur, (i) the S-Pt bond is weakened with the increase of sulfur coverage, (ii) the most stable adsorption site changes from the fcc-hollow site to the atop site, (iii) the energies of the S $2p_{1/2}$ and S $2p_{3/2}$ core levels are very sensitive to the chemical environment and shift to higher binding energy with the increase of S coverage, (iv) compared to the Pt(111) clean surface, the Pt $4f_{5/2}$ and Pt $4f_{7/2}$ core levels are stabilized in energy upon S adsorption, (v) at small sulfur coverages the net charge transfer from Pt to S is minimal, but there is a substantial shift in the Pt $4f$ levels, and (vi) S adsorption induces significant decreases in the density of Pt $5d$ states near the Fermi energy. For the case of adsorption of the S_2 molecule, the S-S bond length is 2.1 Å with one atom near an atop position and the other on a mixed hollow-bridge site. The adsorption energy is close to 44 kcal/mol.

ACKNOWLEDGEMENTS

Work supported by the U.S. DOE (Grant Nos. DE-FG03-99ER14948 and DE-AC02-98CH10886) and by computing time grants from the NERSC.

*Corresponding author. FAX: +1-949-824-2174. Electronic address: wur@uci.edu

[1] J.M. Thomas and W.J. Thomas, *Principles and Practice of Heterogeneous Catalysis* (VCH, New York, 1997).
[2] G.A. Somorjai, *Introduction to Surface Chemistry and Catalysis* (Wiley, New York, 1994).
[3] R.I. Masel, *Principles of Adsorption and Reaction on Solid Surfaces* (Wiley, New York, 1996).
[4] C.H. Bartholomew, P.K. Agrawal, and J.R. Katzer, Adv. Catal. **31**, 135 (1982).
[5] J. Barbier, E. Lamy-Pitara, P. Marecot, J.P. Boitiaux, J. Cosyns, and F. Verna, Adv. Catal. **37**, 279 (1990).
[6] J.A. Rodriguez and J. Hebek, Acc. Chem. Res. **32**, 719 (1999).
[7] J.A. Rodriguez, J. Hrbek, M. Kuhn, and S. Chaturvedi, and A. Maiti, J. Chem. Phys. **113**, 11 284 (2000).
[8] K. Kayek, H. Glassl, A. Gutmann, H. Leonhard, M. Prutton, S.P. Tear, and M.R. Welton-Cook, Surf. Sci. **152/153**, 419 (1985).
[9] W.F. Egelhoff, Surf. Sci. Rep. **6**, 253 (1987).
[10] D.R. Mullins, P.F. Lyman, and S.H. Overbury, Surf. Sci. **277**, 64 (1992) and references therein.
[11] J.A. Rodriguez, S. Chaturvedi, and T. Jirsak, J. Chem. Phys. **108**, 3064 (1998).
[12] J.A. Rodriguez, S. Chaturvedi, and T. Jirsak, Chem. Phys. Lett. **296**, 421 (1998).
[13] E. Wimmer, H. Krakauer, M. Weinert, and A.J. Freeman, Phys. Rev. B **24**, 864 (1981); M. Weinert, E. Wimmer, and A.J. Freeman, Phys. Rev. B **26**, 4571 (1982), and references therein.
[14] M.C. Payne, D.C. Allan, T.A. Arias, and J.D. Johannopoulus, Rev. Mod. Phys. **64**, 1045 (1992).
[15] D. Vanderbilt, Phys. Rev. B **41**, 7892 (1990).
[16] J.A. White and D.M. Bird, Phys. Rev. B **50**, 4954 (1994).
[17] J.P. Perdew, K. Burke, and M. Ernzerhof, Phys. Rev. Lett. **77**, 3865 (1996); J.P. Perdew, K. Burke, and Y. Wang, Phys. Rev. B **54**, 16 533 (1996).
[18] B. Hammer, L.B. Hansen, and J.K. Norskov, Phys. Rev. B **59**, 7413 (1999).
[19] H.J. Monkhorst and J.D. Pack, Phys. Rev. B **13**, 5188 (1976).
[20] J.P. Perdew and Y. Wang, Phys. Rev. B **46**, 6671 (1992).
[21] J.A. Rodriguez, J.M. Ricart, A. Clotet, and F. Illas, J. Chem. Phys. **115**, 454 (2001).
[22] P.J. Feibelman, B. Hammer, J.K. Norskov, F. Wagner, M. Scheffler, R. Stumpf, R. Watwe, and J. Dumesic, J. Phys. Chem. B **105**, 4018 (2001).
[23] V. Milman, B. Winkler, J.A. White, C.J. Pickard, M.C. Payne, E.V. Akhmatskaya, and R.H. Nobes, Int. J. Quantum Chem. **77**, 895 (2000).
[24] X. Lin, N.J. Ramer, A.M. Rappe, K.C. Hass, W.F. Schneider, and B.L. Truot, J. Phys. Chem. B **105**, 7739 (2001).
[25] S.L. Cunningham, Phys. Rev. B **10**, 4988 (1974).
[26] R. Yu, D. Singh, and H. Krakauer, Phys. Rev. B **43**, 6411 (1992).
[27] J.A. Rodriguez, M. Kuhn, and J. Hrbek, Chem. Phys. Lett. **251**, 13 (1996).
[28] F. Illas, A. Clotet, and J.M. Ricart, Catal. Today **50**, 613 (1999).
[29] M.D. Segall, C.J. Pickard, R. Shah, and M.C. Payne, Phys. Rev. B **54**, 16 317 (1996); Mol. Phys. **89**, 571 (1996).
[30] P.J. Feibelman and D.R. Hamann, Surf. Sci. **149**, 48 (1985).
[31] S. Wilke and M. Scheffler, Phys. Rev. Lett. **76**, 3380 (1996).
[32] B. Hammer and J.K. Norskov, Adv. Catal. **45**, 71 (2000).
[33] J.A. Rodriguez and J. Hrbek, J. Phys. Chem. **98**, 4061 (1994).
[34] R. Wu, Chem. Phys. Lett. **238**, 99 (1995); R. Wu and A.J. Freeman, Phys. Rev. B **52**, 12 419 (1995).
[35] E. Pehlke and M. Scheffler, Phys. Rev. Lett. **71**, 2338 (1993).
[36] D. Hennig, M.V. Ganduglia-Pirovano, and M. Scheffler, Phys. Rev. B **53**, 10 344 (1996).
[37] J.A. Rodriguez, J. Dvorak, T. Jirsak, and J. Hrbek, Surf. Sci. **490**, 315 (2001).
[38] M. Kuhn and J.A. Rodriguez, J. Catal. **154**, 355 (1995); J.A. Rodriguez and M. Kuhn, J. Vac. Sci. Technol. A **15**, 1608 (1997).